

N 7 1 - 3 3 5 5 3

NASA TM X-67913

**NASA TECHNICAL  
MEMORANDUM**

NASA TM X-67913

CASE FILE  
CASE FILE  
COPY

**WETTING DYNAMICS OF EVAPORATING  
DROPS ON VARIOUS SURFACES**

by F. F. Simon and Y. Y. Hsu  
Lewis Research Center  
Cleveland, Ohio

TECHNICAL PAPER proposed for presentation at  
Seventieth National Meeting of the American  
Institute of Chemical Engineers  
Atlantic City, New Jersey, August 29-September 1, 1971

# WETTING DYNAMICS OF EVAPORATING DROPS ON VARIOUS SURFACES

by F. F. Simon and Y. Y. Hsu

Lewis Research Center  
National Aeronautics and Space Administration  
Cleveland, Ohio

## SUMMARY

Shape histories of water drops evaporating at room temperature on copper, lucite, stainless steel and teflon were recorded. The drops were observed to go through three stages. In the first stage, the interface radius remained constant while the contact angle reduced with decreasing volume, until the receding angle is reached. In the second stage, the radius decreased almost linearly with time while the contact angle remained a little less than the receding angle. In the third stage, both radius and contact angle reduced rapidly. The relative length of each stage is determined by the type of surface. For a highly wettable surface, Stage I dominated, for a very nonwettable surface, stage II dominated. An analysis is presented enabling the prediction of shape history of a drop provided the evaporation rate and flow resistance over the surface are given.

## INTRODUCTION

The wetting dynamics of an evaporating liquid film is important in determining the efficiency of heat transfer in two-phase flow and the stability of a liquid film in surface coatings. In the annular flow region of two phase flow there is contact of a liquid film with a heated surface. As this film evaporates fluid into the core, a nonwetted surface condition may develop. The growth of nonwetted areas is a limiting condition to good heat transfer in the annular flow regime. Since the initiation and growth of a nonwetted

condition will be determined to a great extent by the wetting nature of the evaporating liquid film on the solid surface, a study of wetting characteristics during evaporation is useful. Another area in which wetting is important during an evaporation process is the stability of liquid surface coatings. Surface coatings such as paints may have a tendency to "crawl" and leave a portion of the surface uncovered. While this situation is initiated by such things as poor surface preparation, evaporation may further increase the tendency of the coating to "crawl". Therefore, the dynamic wetting of an evaporating liquid film as a function of different surface condition is of interest to both situations above.

An index of wetting characteristics is the contact angle. In the case of a static interface, the contact angle is related to the energies at the triple interface line of gas, solid and liquid (Fig. 1(a)). This energy relationship is stated by the following equation of Young and Dupre.\*

$$\gamma_{LV} \cos \theta_e - \gamma_{SV} + \gamma_{SL} = 0 \quad (1)$$

In a dynamic situation where the interface is moving, such as when the liquid is being removed by evaporation, equation (1) is not expected to hold. Under dynamic conditions, the contact angle has to be increased beyond a critical value before the interface will move from a wetted to a nonwetted area. Conversely, an interface would not recede until the contact angle is reduced below a certain angle. These two critical angles are the well-known equilibrium advancing and receding angles. The Young-Dupre equation was

---

\* (See Nomenclature for the definition of symbols.)

modified in Ref. 1 to account for the hysteresis of contact angles as follows:

$$\gamma_{LV}(\cos \theta_r) + C\gamma_{SL} - C\gamma_{SV} - F_r = 0 \quad \text{for receding angle} \quad (2a)$$

$$\gamma_{LV} \cos \theta_a + C\gamma_{SL} - C\gamma_{SV} + F_a = 0 \quad \text{for advancing angle} \quad (2b)$$

The terms  $F_r$  and  $F_a$  account for the additional surface force per unit length that is required for the interface to begin to move (Fig. 1(b)). The energy involved is called "Contortional Energy" by Good (Ref. 2). The coefficient  $C$  is to account for the increase of area due to the presence of roughness.

The equilibrium advancing and receding angles can be measured by tilting a plate to cause the drop to deform until it slides. Another method of obtaining an advancing contact angle is by the addition of fluid to a drop. Conversely a receding angle can be achieved by removal of fluid from a drop. One of the ways of removing liquid is to measure the angle change during evaporation, provided the evaporation rate is extremely slow (Refs. 3 and 4). In Ref. 4, the receding angle was measured by allowing a drop to evaporate and noting the condition at which the drop radius at the solid-liquid interface decreased for constant contact angle. Of special interest to this study are the three stages noted in Ref. 4 which occurred during drop evaporation. At the initiation of drop evaporation the contact angle decreased with time, while the solid-liquid interface radius remained constant (stage I). Stage II became evident when the contact angle remained approximately constant with time (receding contact angle) and the solid liquid interface radius decreased. Stage III occurred at the end of the drop life when both the contact angle and the solid-liquid interface radius decreased with time.

It is the intent of this paper to indicate the variation in interfacial behavior that can be expected from a receding triple-phase line under condi-

tions of evaporation. The contact angles of evaporating water drops on four surfaces with a wide range of wettability were measured. The measured histories of contact angle and the liquid-solid interface radius were compared with an analysis.

#### EXPERIMENTAL METHOD AND PROCEDURE

The basic experimental approach was to record the contact angle and size of an evaporating water drop as a function of time on surfaces of teflon, lucite, copper and stainless steel. Drops were evaporated naturally under ambient conditions. Figure 2 shows the position of the drop with respect to movie camera and to a microscope with a goniometer. The camera was run at a speed of 1 frame every 11 seconds and was synchronized with two electronic light sources. A millimeter scale was placed immediately in back of the drop to provide a length reference. The microscope with the goniometer attachment was used to measure contact angles of the evaporating drops periodically. Although the views of camera and goniometer are perpendicular to each other, the near symmetry of a drop minimized the possible difference in contact angle between the side and front views.

Prior to the runs using copper or stainless substrates, the surfaces were polished. A metallographic polishing procedure was performed which went from a rough grind to a final step of polishing in a vibratory polishing machine with levitated alumina grit. All surfaces were ultrasonically cleaned with mild detergent, rinsed with distilled water and dried with filtered air. The procedures stated above for sample-preparation were followed each time to ensure reproducibility of results from run to run. Reproducibility was important in making independent measurements of receding angle which serve to characterize the surface.

The 16 mm movie films of the evaporating drops were placed in an analyzer that permitted measurement of the projected image. In this way it was possible to obtain the liquid-solid interface radius as a function of time. By using the radius and contact angle information, calculations were made of the volume and evaporation rate.

For the measurements of equilibrium receding angles, the sliding-drop method was used. The deformation and motion of a drop on a slowly tilted surface was recorded by motion pictures from which the receding angles were measured.

## RESULTS

### Experimental Data

Typical curves of liquid-solid interface radius and contact angle against time during drop evaporation are shown in Figs. 3-6. These figures are arranged in the order of increasing receding contact angles; namely, water-copper, water-lucite, water-stainless steel, and water-teflon. With exceptions to be discussed later, these figures have features common to those discussed in Ref. 2. An idealized model for the general behavior is depicted in Fig. 7. First, in the early stages of evaporation there is a constant radius period in conjunction with a decreasing contact angle (Stage I). Then, one may observe in some cases a second stage (Stage II) in which the contact angle is nearly constant but the radius is decreasing almost linearly with time. Then there is the last stage (Stage III) in which both radius and contact angle decrease rather rapidly with time. The lengths of the various

stages depend upon the rate of evaporation and the size of the receding angle. All the surfaces studied except copper exhibited the three stages indicated above. A water drop on copper exhibited Stage I for the majority of the drop life. Representative photographs from the movie film of the teflon and copper surfaces are shown in Figs. 8 and 9. These pictures demonstrate the fact that a teflon surface permits a long Stage-II event while an evaporating drop on copper is primarily a Stage-I phenomenon.

### Analysis

In order to describe the variation of drop size with time during evaporation, a model is proposed as follows:

(1) The shape of a sessile drop is really not a truncated sphere and cannot be stated in explicit form. However, for simplicity a truncated sphere geometry is assumed to represent the drop shape. (See Fig. 1.)

$$V = \frac{\pi}{3} R^3 (1 - \cos \theta)^2 (2 + \cos \theta) = \frac{\pi}{3} r^3 \frac{(1 - \cos \theta)^2 (2 + \cos \theta)}{\sin^3 \theta} \quad (3)$$

with

$$R = \frac{r}{\sin \theta} \quad (4)$$

It is found that by comparing the true volume of a drop with that for a truncated sphere, an error of about 5 percent results.

(2) The drop volume is reduced due to evaporation by the rate

$$\frac{dV}{dt} = -\Gamma S \quad (5)$$

with the drop surface  $S$  defined as

$$S = \frac{2\pi r^2}{\sin^2 \theta} (1 - \cos \theta) \quad (6)$$

When the drop volume is reduced, the volume change has to be accomplished by either reduction of angle or radius, or both:

$$\frac{dV}{dt} = \left. \frac{\partial V}{\partial \theta} \right|_r \frac{d\theta}{dt} + \left. \frac{\partial V}{\partial r} \right|_\theta \frac{dr}{dt} \quad (7)$$

$$-\Gamma S = \left. \frac{\partial V}{\partial \theta} \right|_r \frac{d\theta}{dt} + \left. \frac{\partial V}{\partial r} \right|_\theta \frac{dr}{dt} \quad (8)$$

Using equation (8) and the partial derivatives from equation (3), the following relation between  $r$  and  $\theta$  as function of time  $t$  can be obtained.

$$-2\Gamma = \frac{(1 - \cos \theta)}{\sin^2 \theta} \left[ (2 + \cos \theta) \sin \theta \frac{dr}{dt} + r \frac{d\theta}{dt} \right] \quad (9)$$

The solution of equation (9) depends on the relation between  $r$  and  $\theta$  which can be described by the stages of evaporation:

(a) Stage I:

$$\left. \begin{array}{l} \frac{dr}{dt} = 0 \\ \theta \geq \theta_r \end{array} \right\} \quad (10)$$

when

and

$$r = \text{const} = r_0 \quad (10a)$$

Thus the solution is simple

(b) Stage II and III: The relation between  $r$  and  $\theta$  is supplied by a force balance to be discussed as follows.

Recall in equation (2) that for the equilibrium receding angle, a surface force  $F_r$  was required for an interface to begin to move. When the drop is evaporating and its radius is reducing at a finite rate, there is an actual flow of liquid which is more than the infinitesimal rate implied in the receding angle equations. An additional force is required to effect the flow. Although it is theoretically possible to determine the shear stress required to cause this flow by considering the basic momentum and continuity equations, it is assumed that the additional force required is proportional to the time rate of change of the liquid-solid interface radius (Fig. 10). Essentially, this model assumes a linear velocity profile or an analogy to the Couette type of flow. Figure 10 can be compared with Fig. 1(a) and 1(b).

$$F_f = -f \frac{dr}{dt} \quad (11)$$

or, the force-balance equation is modified to read:

$$\gamma_{LV} \cos \theta + C\gamma_{LS} = C\gamma_{SV} + F_r - f \frac{dr}{dt} \quad (12)$$

Note that when  $dr/dt \rightarrow 0$ , equation (12) is reduced to equation (2) which is the case when the interface just begins to move. Substraction of equation (2) from the above equation results in:

$$\gamma_{LV}(\cos \theta - \cos \theta_r) = -f \frac{dr}{dt} \quad (13)$$

Differentiation of equation (13) yields:

$$\gamma_{LV} \sin \theta \frac{d\theta}{dt} = f \frac{d^2r}{dt^2} \quad (14)$$

thus

$$\frac{d\theta}{dt} = \frac{f}{\gamma_{LV} \sin \theta} \frac{d^2 r}{dt^2} \quad (15)$$

with the boundary conditions:

$$r = r_0, \quad \frac{dr}{dt} = 0$$

at

$$\theta = \theta_r$$

Equation (15) is the relation between  $r$  and  $\theta$  needed for the completion of the governing equations.

Elimination of  $d\theta/dt$  between equation (9) and (15) yields:

$$-2\Gamma \sin^3 \theta = \frac{f}{\gamma_{LV}} (1 - \cos \theta) r \frac{d^2 r}{dt^2} + (1 - \cos \theta)(2 + \cos \theta) \sin^2 \theta \frac{dr}{dt} \quad (16)$$

The initial condition for Stage-II is

$$t = t_{II,0}, \quad r = r_0, \quad r_{II,0}^{\dot{}} = 0, \quad \theta = \theta_r \quad (17)$$

Thus a complete solution for  $r$  and  $\theta$  in Stage-II requires the simultaneous solution of equations (16), (3), and (5). However, since equation (16) is a function of  $r$  and  $\theta$ , it appears that equation (16) and (17) can be used to solve for  $r(t)$  if  $\theta(t)$  is known. Thus, if a proper  $\theta(t)$  curve can be assumed, an approximation for  $r(t)$  can be obtained which then can be used as an input to an iterative scheme for the complete solution.

### Approximate Solutions

The inputs needed for solution of equation (16) are:

- (1) Evaporation Coefficient  $\Gamma$
- (2) Resistance Coefficient  $f$
- (3) Time history of contact angle  $\theta(t)$
- (4) Initial slope of radius  $r'$   
 $\text{II, } 0$

Of the four items,  $\Gamma$  and  $f$  are parameters. Theoretically, they should be obtainable through basic consideration of energy and momentum transport. For lack of simple solutions, we can use empirical values obtained from experimental results of  $r(t)$  and  $V(t)$ , with the understanding that eventually they should be obtained a priori. It should be noted that although empirical values of  $f$  are fairly constant over the majority of Stage II, the empirical evaporation coefficient  $\Gamma$  does vary by a factor of 2 with drop size. Therefore there is the option of using a mean value of  $\Gamma$ , (i. e.,  $\Gamma_{\text{mean}}$ ), or using  $\Gamma$  as function of time  $\Gamma(t)$ .

The third item of the input,  $\theta(t)$ , is the functional relation of contact angle with time. It can be either the result of a complete solution, as mentioned in the last section, or an approximate form can be used as input for iteration. There are two possible choices. First is to use the experimentally determined history of  $\theta$ , i. e.,  $\theta_{\text{exp}}(t)$ . The second possibility to assume  $\theta = \theta_r$  since this is approximately the case for the main part of Stage II.

Item four is the initial value of  $r'_0$  at the beginning of Stage II. Theoretically,  $r'_0$  should be zero but experimentally, it is finite.

#### Comparison of Experimental Results with Approximate Solutions

For the comparison of experimental results with analysis, we can ignore Stage I since it is simply a constant radius region. The important test is after the beginning of Stage II.

In order to check the analysis and its approximations for Stages II and III, machine computations were made using equation (16). The analytical results of Fig. 4(a) were made by using experimental values of  $\theta(t)$ ,  $r'_0$ ,  $f$  and  $\Gamma(t)$  as input to obtain radius against time curves. The agreement of the computed values with the experimental data shows that the analytical model is realistic. Additional simplifications can be introduced to make the model more practical. To show the effect of assuming  $r'_0 = 0$  at the beginning of Stage II, two curves using  $r'_0 = 0$  and  $r'_0 = -6.93 \times 10^{-5}$  cm/sec (experimental value) were obtained by use of equation (16) with the experimental value to  $\theta(t)$  as input. The result is shown in Fig. 6(a). As the results show, the assumption of  $r'_0 = 0$  will introduce an error of about 5 percent on the average for the life time of the drop.

To test the assumption of using  $\theta = \theta_r$  and also  $\Gamma = \Gamma_{\text{mean}}$  three curves were generated for the following conditions:

$$\theta = \theta_{\text{exp}}(t) \quad \Gamma = \Gamma_{\text{exp}}(t) \quad r'_0 = 0$$

$$\theta = \theta_{\text{exp}}(t) \quad \Gamma = \Gamma_{\text{mean}} \quad r'_0 = 0$$

$$\theta = \theta_r \quad \Gamma = \Gamma_{\text{mean}} \quad r'_0 = 0$$

The comparisons are shown in Fig. 5. The comparisons show that the first

order approximation of assuming  $\theta = \theta_r$  and  $\Gamma = \Gamma_{\text{mean}}$ ,  $r'_0 = 0$  does not cause great deviation from the experimental data.

#### ADDITIONAL OBSERVATIONS AND DISCUSSION

In Stage II, the contact angle departs slightly from its equilibrium receding value prior to the movement of the triple interface line. This departure is not always small as can be seen in the curve for teflon (Fig. 6) at a time of 1000 seconds. The teflon curve also dramatizes the recovery back to the receding contact angle. Apparently, the liquid drop is stressed prior to the movement of the triple interface line. In Stage III there is no recovery to a receding contact angle. A possible cause for this is that the ratio of surface area to volume has become large, causing a more rapid decrease in volume than occurred in phase II. This rapid volume decrease does not permit sufficient time for recovery of the drop contact angle.

The equilibrium receding angle, measured by the sliding-drop method are indicated on Fig. 3-6 for comparison with the evaporating drops. With the exception of stainless steel, the sliding-drop receding contact angles are consistent with the evaporating drop results. For the case of lucite (Fig. 4(b)) and teflon (Fig. 6(b)) there is little difference between the receding angle of the sliding drop and the Stage-II contact angle. This small difference is to be expected because of the very low but finite evaporation rate. Therefore, the evaporating drop is a satisfactory method for measuring receding contact angle provided the evaporation rate is sufficiently low.

In our experiments a water drop on a copper surface did not go through a Stage II performance. The drop history during Stage II is dependent on the receding contact angle. This suggests that the receding contact angle for our copper surface was so low that by the time this angle was reached the Stage III effects dominated the drop life. The receding angle from sliding-drop method verifies this explanation (Fig. 3(b)).

### CONCLUSIONS

From the experimental results and analysis, the following conclusions can be reached.

1. The change of shape of an evaporating drop is dependent upon the type and condition of the solid surface and on the evaporation rate with the receding angle as a controlling factor. In the extreme cases, the drop radius remains constant while the contact angle decreases continuously for a highly wettable surface, while for a highly nonwetting surface, the contact angle remains close to the equilibrium receding angle and the radius shrinks.

2. The shape history of a drop as described in Ref. 2 for limited cases are found to be applicable to a wide range of surface conditions. It can be qualitatively described as composed of three stages:

Stage I contact angle  $\theta \geq$  equilibrium receding angle  $\theta_r$ ,  $r = r_0$

Stage II  $\theta < \theta_r$ ,  $r < r_0$

Stage III  $\theta$  and  $r$  rapidly approach zero

3. An analysis has been conducted to predict the shape and size history. A first approximation can be obtained by use of a few simplified assumptions. Comparison of experimental data with the computations show that these approximations permit close agreement with the experimental results.

4. It should be cautioned that when the method of evaporating drop is used to measure the receding angle, the evaporation rate should be extremely slow. Otherwise, an angle smaller than the true receding angle (Stage II) will be obtained.

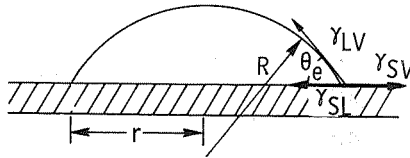
## APPENDIX - SYMBOLS

|                 |  |
|-----------------|--|
| C               | roughness coefficient  |
| $F_a$           | surface force per unit length, or contortional energy, needed to start the advancing of an interface |
| $F_f$           | surface force per unit length resisting the motion of interface                                      |
| $F_r$           | surface force per unit length, or controtional energy, needed to start the receding of an interface  |
| f               | coefficient associated with $F_f$  |
| R               | radius of curvature  |
| r               | contact radius   |
| $r_o$           | initial contact radius   |
| $r'$            | = $dr/dt$  |
| S               | liquid-vapor surface area of the drop  |
| t               | time   |
| $t_{II,o}$      | time at beginning of Stage II  |
| V               | volume of the drop   |
| $\Gamma$        | evaporation coefficient  |
| $\Gamma_{mean}$ | mean value of evaporation coefficient  |
| $\gamma_{LV}$   | interfacial tension between liquid and vapor   |
| $\gamma_{SL}$   | interfacial tension between solid and liquid   |
| $\gamma_{SV}$   | interfacial tension between solid and vapor  |
| $\theta$        | contact angle  |
| $\theta_a$      | advancing contact angle  |
| $\theta_e$      | static contact angle with interfacial tensions in equilibrium  |
| $\theta_r$      | receding contact angle   |

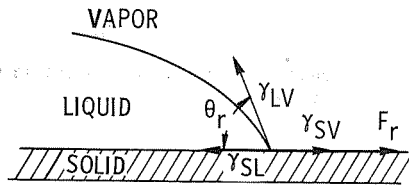
## REFERENCES

1. Adam, W. K., and Jessop, G., J. Chem. Soc., 127, 1863 (1925).
2. Good, R. J., J. Am. Chem. Soc., 74, 5041 (1952).
3. Herzberg, W. J., and Marian, J. E., J. Colloid Interface Sci., 33, 161 (1970).
4. Herzberg, W. J., Marian, J. E., and Vermeulen, T., J. Colloid Interface Sci., 33, 164 (1970).

E-6535



(A) GEOMETRICAL REPRESENTATION OF A DROP WITH TRIPLE INTERFACE VECTORS.



(B) FORCE BALANCE FOR AN EQUILIBRIUM RECEDING ANGLE.

Figure 1

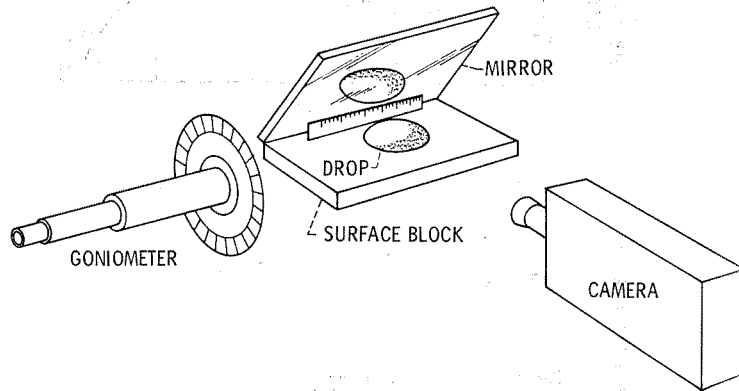


Figure 2. - Apparatus configuration.

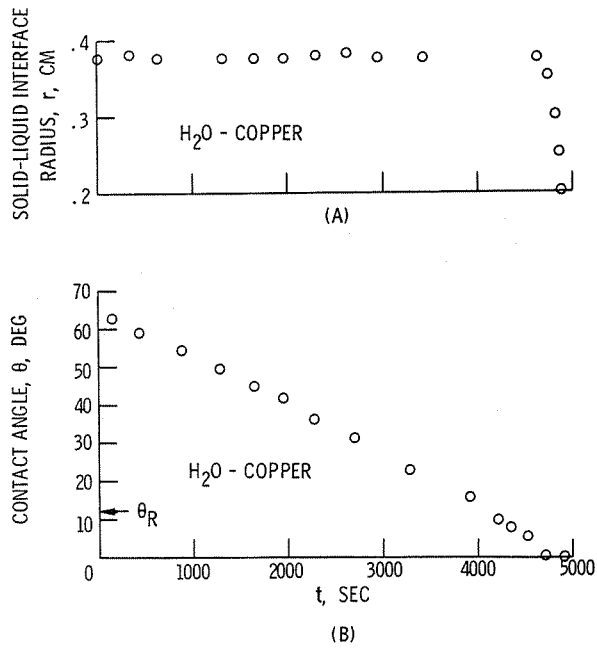


Figure 3. - Shape history of a drop, radius and contact angle.

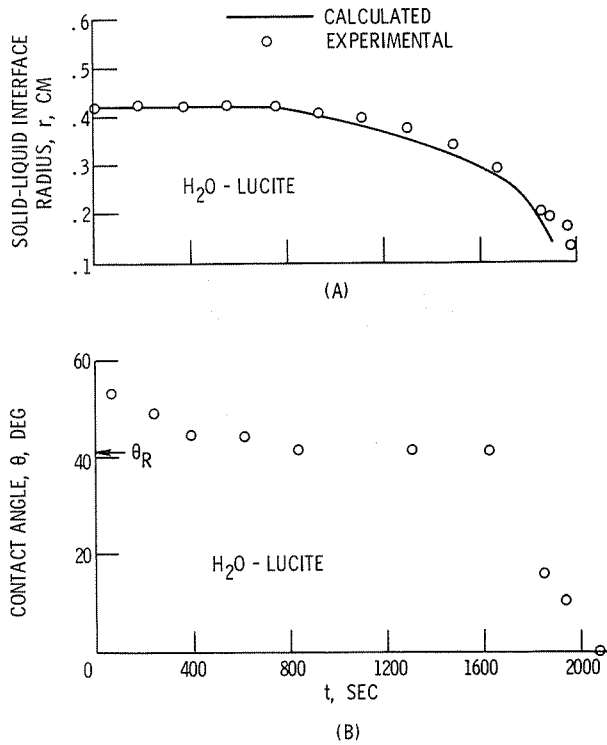


Figure 4. - Shape history of a drop, radius and contact angle.

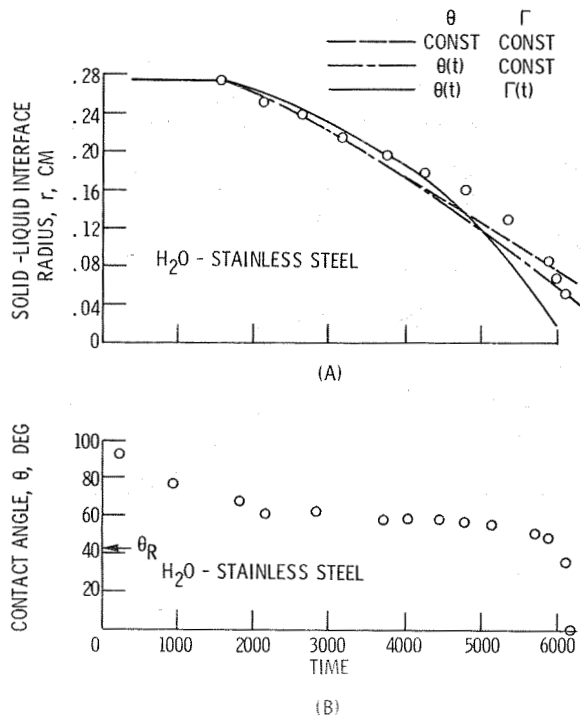


Figure 5. - Shape history of a drop, radius and contact angle.

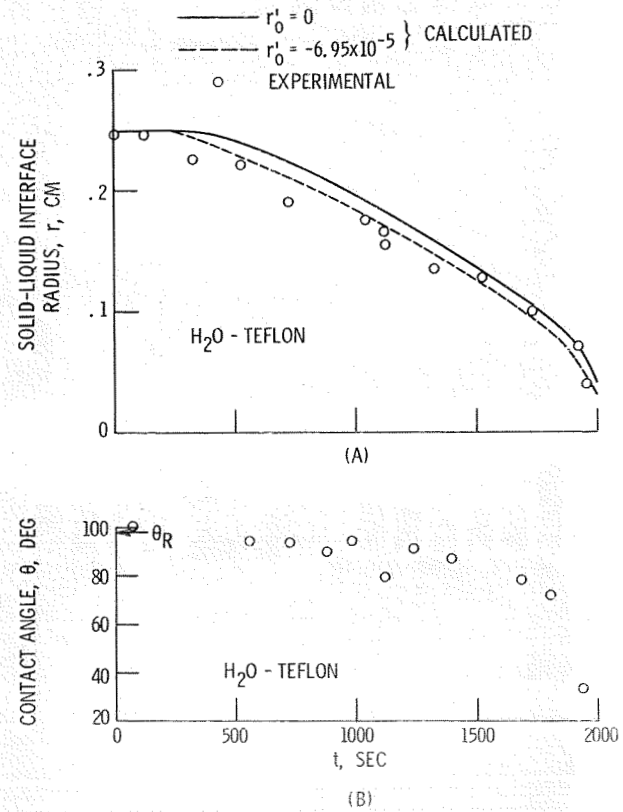


Figure 6. - Shape history of a drop, radius and contact angle.

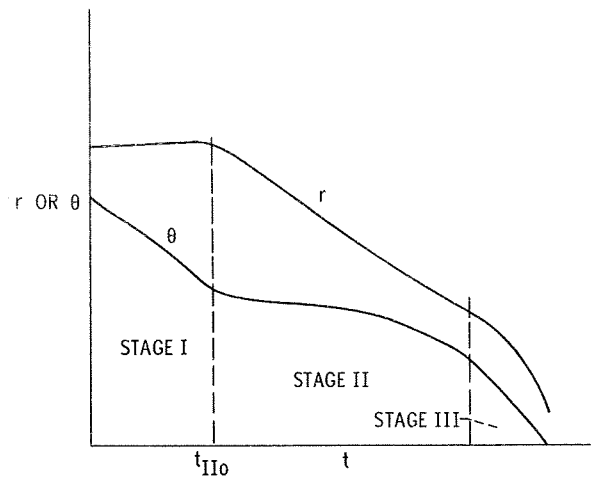
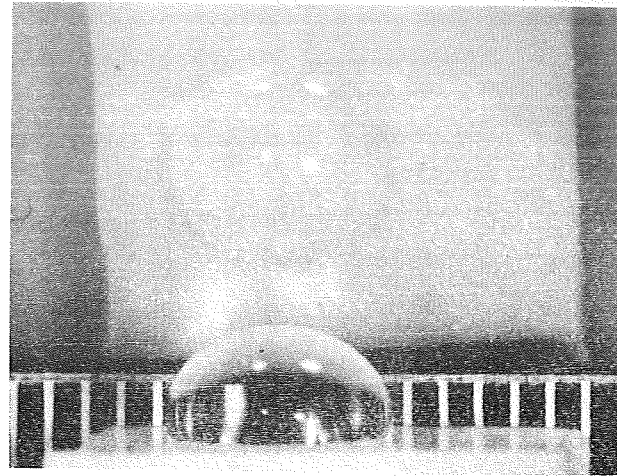
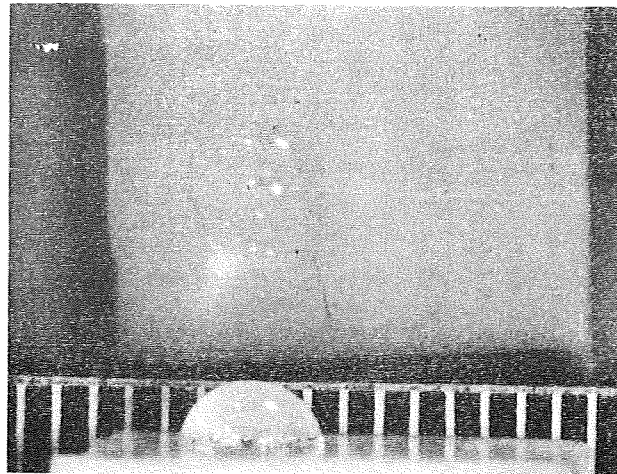


Figure 7. - Idealized history of radius and contact angle variation for an evaporating drop.

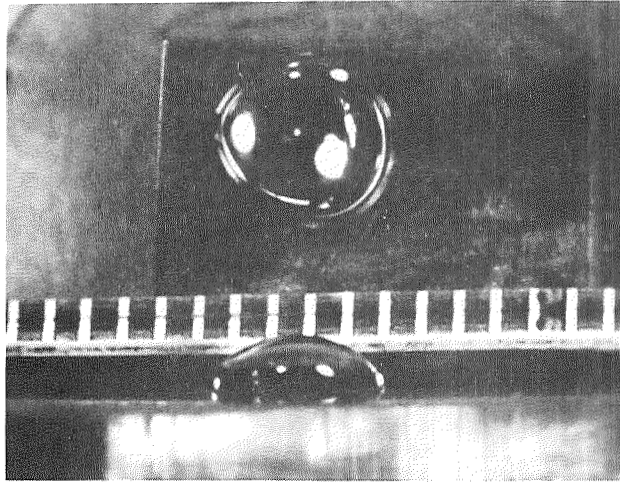


t = 0 SEC

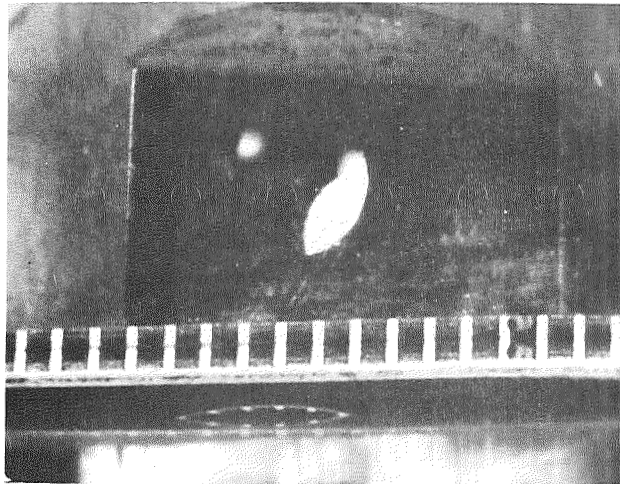


t = 1560 SEC

Figure 8. - Evaporation of a water drop on a teflon surface.



t = 81 SEC



t = 4050 SEC

Figure 9. - Evaporation of a water drop on a copper surface.

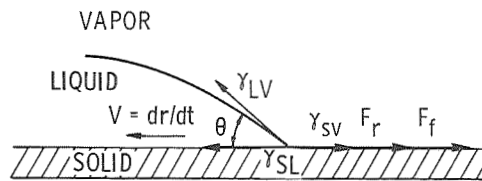


Figure 10. - Force balance on a moving interface (eq. (9)).